

Anisotropic broadening of Cu nanorods during glancing angle deposition

S. V. Kesapragada and D. Gall^{a)}

Department of Materials Science and Engineering, Rensselaer Polytechnic Institute, Troy, New York 12180

(Received 9 August 2006; accepted 3 October 2006; published online 17 November 2006)

Regular arrays of freestanding Cu nanostructures were grown on patterned Si substrates using glancing angle deposition (GLAD) from two oppositely positioned sputtering sources. Continuous azimuthal substrate rotation during deposition leads to the formation of vertical 430-nm-wide rods, which broaden anisotropically during subsequent growth with a stationary substrate. Statistical analyses of plan-view micrographs combined with numerical simulations indicate a linear increase in the width aspect ratio with deposition time that is attributed to a change in the growth front direction. This technique, termed simultaneous opposite GLAD, provides a unique approach for nanostructure shaping. © 2006 American Institute of Physics. [DOI: 10.1063/1.2388861]

Glancing angle deposition (GLAD) has gained considerable interest in recent years due to its ability to create arrays of uniquely shaped nanostructures built from a wide range of material systems.¹⁻³ It exploits atomic shadowing effects during line-of-sight physical vapor deposition by controlling polar α and azimuthal φ deposition angles to nanoengineer columns into various shapes such as zigzags,⁴ pillars,⁵ chevrons,⁶ spirals,⁷ slanted posts,⁸ multistack columns,⁹ flowers,¹⁰ and Y shapes,^{11,12} with potential applications as optically active layers,^{13,14} magnetic storage media,^{6,15} humidity and pressure sensors,^{16,17} emitters,¹⁸ and actuators.¹⁹ Most reported studies on GLAD use a single deposition source and control the nanocolumn shapes by complex cyclic substrate rotations about α and φ . An additional promising approach for lateral nanostructuring, as investigated here, is the simultaneous use of multiple deposition sources during GLAD, which is expected to result in layers with highly anisotropic electric and optical properties and has been shown to yield a columnar alignment parallel to the evaporation plane during Co-Cr codeposition.²⁰

In this letter, we demonstrate that the simultaneous deposition from opposite sides onto a stationary substrate can be exploited to control lateral column shapes and cause anisotropic broadening in GLAD nanostructures. This technique, called simultaneous opposing GLAD (SOGLAD), is applied on regular arrays of Cu nanorods that were grown on patterned Si substrates. A numerical model shows that the anisotropic broadening during SOGLAD can be explained by a change in the average growth front direction, causing a net lateral growth component.

All Cu nanorods were grown in a load-locked ultrahigh vacuum magnetron sputter deposition system on Si (001) substrates that were patterned with 500-nm-diameter polystyrene microspheres that self-assemble from colloidal suspensions into hexagonal close-packed monolayers.^{21,22} The substrate was placed in the center of two 7.5-cm-diameter Cu targets (99.95% pure) that were facing each other and were separated by 20 cm, with the plane of the substrate surface perpendicularly intersecting both target centers. A 38-mm-diameter collimating plate was positioned parallel to the substrate surface at a distance of 3 mm, in order to prevent any nondirectional flux from striking the substrate, and

to control the polar deposition angle to be 84°. ⁹ The two step growth process consisted of (1) deposition with continuous substrate rotation with 50 rpm about the polar axis, leading to vertical columns, followed by (2) deposition from opposite sides onto a stationary substrate to investigate the morphological evolution during SOGLAD. Sputtering was carried out in a 0.26 Pa (2.0 mTorr) 99.999% pure Ar atmosphere that was further purified using a Micro Torr purifier. A fixed power of 750 W on each target resulted in a column growth rate of 50 nm/min. The substrate temperature, measured by a thermocouple attached to the substrate holder, increased from room temperature to 140 °C, due to heating from the plasma discharge.

Figure 1(a) is a scanning electron micrograph of 1.5- μm -tall Cu nanorods grown by GLAD with continuous substrate rotation onto a self-organized monolayer of polystyrene spheres on Si(001). The micrograph was obtained with the electron beam of the SEM tilted by an angle of 45° with respect to the substrate surface normal, providing a “bird’s view” image. The nanorods are oriented perpendicular to the substrate surface and form a hexagonal close-packed array, replicating the structure of the initial substrate pattern. Their average center-to-center separation is 496 ± 32 nm, close to the nominal diameter of the polystyrene spheres of 500 nm. Their width is 432 ± 31 nm and remains approximately constant as a function of height, indicating negligible intercolumnar growth competition. The Cu rods exhibit faceting, which allows to determine their crystalline structure, as described in detail in Ref. 11. Most of them are $\langle 110 \rangle$ -, $\langle 001 \rangle$ -, or $\langle 111 \rangle$ -oriented single crystals, while others are polycrystalline, exhibit multiple stacking faults, and/or branch into complex morphologies.¹¹

Figures 1(b) and 1(c) show SEM micrographs of Cu nanostructures grown by SOGLAD onto vertical 1.5- μm -tall rods. That is, first, nanorods comparable to those shown in Fig. 1(a) were grown using continuous substrate rotation. Secondly, growth was continued with a stationary substrate using simultaneously two deposition sources which, within the coordinates of the micrographs, are located to the left and the right. The deposition time for SOGLAD was chosen such that it corresponds to additional nominal nanorod heights of 0.25 and 0.50 μm , for Figs. 1(b) and 1(c), respectively. The micrographs, obtained with a 45° tilt, show a cross-section-like view of the Cu nanostructures that exhibit wide tops on narrower rods, indicating a rod broadening during SOGLAD.

^{a)}Electronic mail: galld@rpi.edu

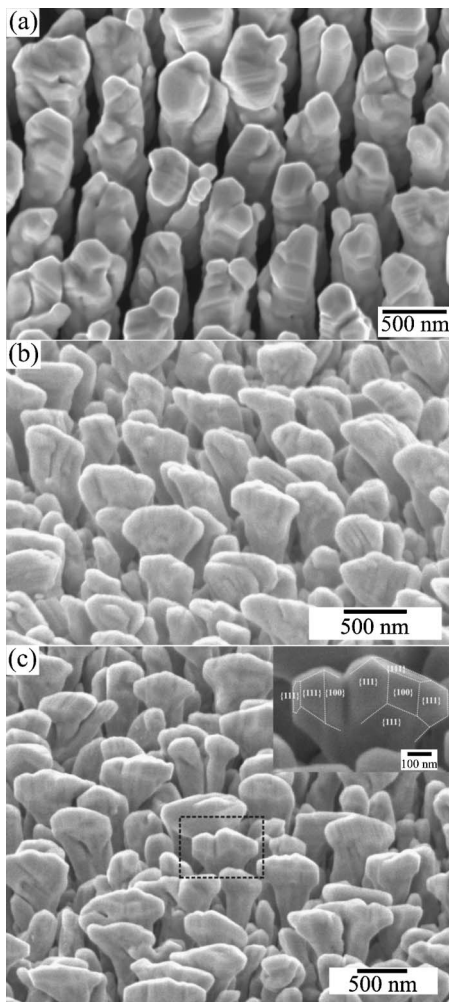


FIG. 1. (a) SEM image of 1.5- μm -tall Cu nanorods grown with continuous substrate rotation, and micrographs from samples exposed to an additional (b) 0.25 μm and (c) 0.50 μm stationary flux from two opposing sources (SOGLAD). The inset in (c) is a higher magnification image with highlighted facet boundaries.

The average measured widths on the top, which range from 500 to 670 nm for Fig. 1(b) and from 550 to 1080 nm for Fig. 1(c), are considerably larger than the initial rod diameter [from Fig. 1(a)] of 432 nm. Despite the broadening, the nanostructures are freestanding and do not touch their neighbors. This is attributed to a competitive growth mode²² during SOGLAD, which causes a considerable fraction of the nanorods to die out. That is, while some (slightly higher) rods broaden, neighboring rods are overshadowed and their growth is terminated, causing an overall reduction of the nanorod number density to 71% and 46% of the original rod density for 0.25 and 0.50 μm of SOGLAD, respectively, as quantified using plan-view micrographs.

The inset in Fig. 1(c) is a high magnification image of the nanostructure that is enclosed by a dashed rectangle in Fig. 1(c). It indicates the strong tendency for faceting along low-energy $\{111\}$ and $\{100\}$ planes, as observed for all Cu rods in Fig. 1. The nanostructure is an example illustrating how faceting affects atomic shadowing and microstructural evolution during SOGLAD. The structure exhibits branching, caused by the development of a vertical groove and a surface cusp near the middle of the structure, which we attribute to the combination of a local growth suppression due to atomic shadowing and a relatively high three-dimensional

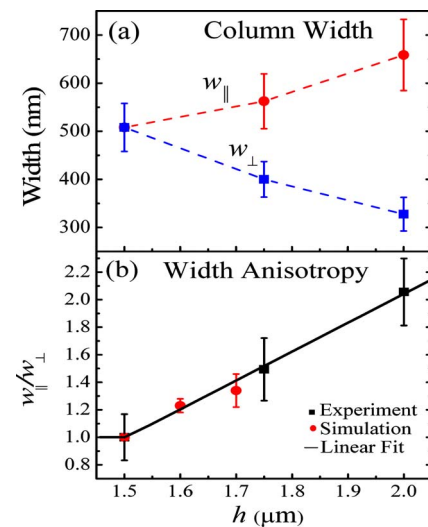


FIG. 2. (Color online) (a) Width parallel w_{\parallel} and perpendicular w_{\perp} to the SOGLAD deposition flux vs the nominal Cu nanorod height h , where substrate rotation was halted at $h=1.5 \mu\text{m}$, (b) corresponding width aspect ratio.

Ehrlich-Schwöbel barrier for adatom migration over facet edges.²³

Figure 2(a) is a plot of the average width of the nanorods in the direction parallel (w_{\parallel}) and perpendicular (w_{\perp}) to the SOGLAD flux versus the nominal rod height h . The values of w_{\parallel} and w_{\perp} are determined using statistical analyses of plan-view micrographs. $w_{\parallel}=w_{\perp}$ for $h \leq 1.5 \mu\text{m}$, since the rods are grown up to this height with continuous substrate rotation. The width at $h=1.5 \mu\text{m}$ is $508 \pm 43 \text{ nm}$. This is slightly larger than $432 \pm 31 \text{ nm}$, the value measured using cross-sectional micrographs, indicating a systematic overestimation of the width by plan-view micrographs²² related to protrusions and short side branches that make the rod appear wider than its average width.¹¹ For $h > 1.5 \mu\text{m}$, w_{\parallel} and w_{\perp} show opposite trends: w_{\parallel} increases from 508 to 658 nm, indicating a rod broadening along the SOGLAD deposition direction, while w_{\perp} decreases to 327 nm, indicating a corresponding reduced growth rate perpendicular to the deposition flux. Figure 2(b) is a plot of the width aspect ratio (w_{\parallel}/w_{\perp}), indicating a linear increase in the rod broadening within the investigated range from 1.0 prior to initiating SOGLAD to 2.05 ± 0.24 for a nominal deposition of 0.5 μm of SOGLAD. The plot also includes data from the numerical simulation described below, showing excellent agreement with our experimental result.

We numerically simulate the initial stages of the morphological evolution during SOGLAD, including the anisotropic broadening, as follows. The local growth rate $g(\alpha, \theta, \varphi)$ in the direction perpendicular to the substrate surface at a point p on a nanocolumn is determined by the polar deposition angle $\alpha=84^\circ$, the angle θ between the local surface and the substrate surface, and the azimuthal angle φ by

$$g(\alpha, \theta, \varphi) = \frac{\cos \gamma}{\cos \theta} f(h), \quad (1)$$

where

$$\cos \gamma = \sin \alpha \sin \theta \cos \varphi + \cos \alpha \cos \theta. \quad (2)$$

Here γ is the angle between the deposition flux and the local surface normal and $f(h)$ is the deposition rate as a function of

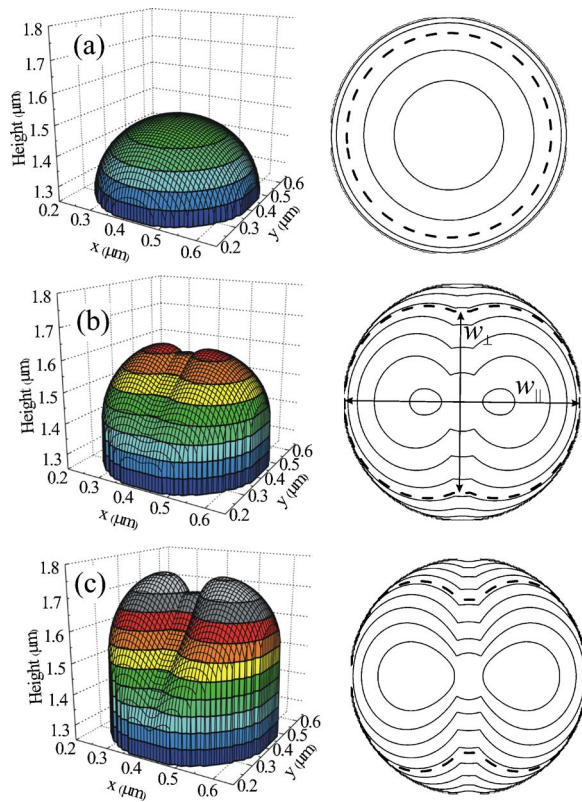


FIG. 3. (Color online) Plot of simulated morphologies and corresponding contour plots of the top-portion of 500 nm diameter nanorods grown with (a) continuous substrate rotation and with additional (b) 100 nm and (c) 200 nm of SOGLAD.

height. $f(h)$ accounts for the shadowing from neighboring columns and is assumed to be a global function, that is, it is independent on the local geometry of the intercolumn arrangements. For deposition with continuous rotation about the azimuthal angle φ , the nanocolumn is expected to be circular symmetric. In that case, the growth G during a 360° rotation depends only on the distance r between p and the symmetry axis of a growing nanocolumn,

$$G(r) = \frac{1}{2\pi} \int_{-\varphi_0}^{\varphi_0} g(\alpha, \theta, \varphi) d\varphi, \quad (3)$$

where $\varphi_0 = (\cos \alpha \cos \theta) / (\sin \alpha \sin \theta)$ is the critical azimuthal angle for deposition, which is determined using Eq. (2) and the requirement that deposition at a specific point on the nanocolumn surface occurs only if $\gamma < 90^\circ$.

We now assume that the Cu nanorods exhibit a constant width during growth with continuous rotation, as observed experimentally in Fig. 1(a). This means that the column growth during continuous rotation is independent of r , that is, $G(r) = G_0$. The function $f(h)$ can then be analytically determined using Eqs. (1)–(3), a given constant G_0 , and assuming a spherically shaped column tip, as illustrated in Fig. 3(a). The growth rate for a stationary substrate and deposition from two sources corresponding to the experimental arrangement is then calculated using Eqs. (1) and (2) and $f(h)$. The result is illustrated in Figs. 3(b) and 3(c), which show the top portion of the expected column morphology for 500-nm-wide columns with an additional 100 and 200 nm of SOGLAD, respectively.

The column-tip morphology prior to SOGLAD is spherical, as indicated in Fig. 3(a) by the perfect circles in the

contour plot. The dashed line in this plot corresponds to the tip shape at half-height, which is used to determine the width aspect ratio $w_{\parallel}/w_{\perp} = 1$. The aspect ratio increases to 1.23 ± 0.05 and 1.34 ± 0.12 for 100 and 200 nm of SOGLAD, respectively. These values are also shown as data points in Fig. 2(b), indicating an excellent agreement of the model and the experimental observation. The good agreement is particularly notable, since the experimentally observed faceting and branching are not simulated. In addition, the model is expected to deviate from experiment for larger growth times, since it assumes a spherical column-tip shape for the determination of the local growth rate, which is no longer true if the column morphology is deformed by the anisotropic lateral growth during SOGLAD. Nevertheless, the simple model correctly describes the initial stages of the anisotropic broadening, the lateral growth during SOGLAD, as well as the growth suppression in the direction perpendicular to the deposition flux. Figure 3(c) even qualitatively resembles the inset in Fig. 1(c), showing a surface cusp as well as a vertical groove.

In summary, growth experiments and numerical modeling show that nanocolumns broaden anisotropically when substrate rotation is stopped during GLAD with two oppositely positioned sources. The broadening is attributed to a change in the direction of the growth front from straight up to lateral growth, leading to an increase of the nanorod width in the direction parallel to the SOGLAD flux and a decrease in the perpendicular direction, resulting in an overall linear increase in the width aspect ratio.

This research was supported by the National Science Foundation, Division of Manufacturing and Industrial Innovation, under Grant No. DMII-0423358.

- ¹K. Robbie, M. J. Brett, and A. Lakhtakia, *Nature (London)* **384**, 616 (1996).
- ²R. Messier, V. C. Venugopal, and P. D. Sunal, *J. Vac. Sci. Technol. A* **18**, 1538 (2000).
- ³K. Robbie, D. J. Broer, and M. J. Brett, *Nature (London)* **399**, 764 (1999).
- ⁴K. Robbie and M. J. Brett, *J. Vac. Sci. Technol. A* **15**, 1460 (1997).
- ⁵B. Dick, M. J. Brett, and T. Smy, *J. Vac. Sci. Technol. B* **21**, 2569 (2003).
- ⁶B. Dick, M. J. Brett, T. J. Smy, M. R. Freeman, M. Malac, and R. F. Egerton, *J. Vac. Sci. Technol. A* **18**, 1838 (2000).
- ⁷S. R. Kennedy and M. J. Brett, *J. Vac. Sci. Technol. B* **22**, 1184 (2004).
- ⁸D.-X. Ye, T. Karabacak, R. C. Picu, G.-C. Wang, and T.-M. Lu, *Nanotechnology* **16**, 1717 (2005).
- ⁹S. V. Kesapragada and D. Gall, *Thin Solid Films* **494**, 234 (2006).
- ¹⁰Y.-P. Zhao, D.-X. Ye, G.-C. Wang, and T.-M. Lu, *Nano Lett.* **2**, 351 (2002).
- ¹¹J. Wang, H. Huang, S. V. Kesapragada, and D. Gall, *Nano Lett.* **5**, 2505 (2005).
- ¹²C. M. Zhou and D. Gall, *Appl. Phys. Lett.* **88**, 203117 (2006).
- ¹³M. Suzuki and Y. Taga, *J. Appl. Phys.* **71**, 2848 (1992).
- ¹⁴I. J. Hodgkinson and Q. H. Wu, *Opt. Eng. (Bellingham)* **37**, 2630 (1998).
- ¹⁵A. Lisfi and J. C. Lodder, *Phys. Rev. B* **63**, 174441 (2001).
- ¹⁶J. J. Steele, A. C. van Popta, M. M. Hawkeye, J. C. Sit, and M. J. Brett, *Sens. Actuators B* (2006).
- ¹⁷S. V. Kesapragada, P. Victor, O. Nalamasu, and D. Gall, *Nano Lett.* **6**, 854 (2006).
- ¹⁸J. P. Singh, F. Tang, T. Karabacak, T.-M. Lu, and G.-C. Wang, *J. Vac. Sci. Technol. B* **22**, 1048 (2004).
- ¹⁹J. P. Singh, D.-L. Liu, D.-X. Ye, R. C. Picu, T.-M. Lu, and G.-C. Wang, *Appl. Phys. Lett.* **84**, 3657 (2004).
- ²⁰H. V. Kranenburg, J. C. Lodder, Y. Maeda, L. Toth, and Th. J. A. Popma, *IEEE Trans. Magn.* **26**, 1620 (1990).
- ²¹R. Micheletto, H. Fukuda, and M. Ohtsu, *Langmuir* **11**, 3333 (1995).
- ²²C. M. Zhou and D. Gall, *Thin Solid Films* **515**, 1223 (2006).
- ²³J. Wang, H. Huang, and T. S. Cale, *Modell. Simul. Mater. Sci. Eng.* **12**, 1209 (2004).